

Theoretical Study on the Disproportionation Reaction of Nickel(II) Mixed-Ligand Complexes Containing *N*,*N*,*N*′,*N*′-Tetramethylethylenediamine, Benzoylacetonate, and a Halide Anion

Keiko Miyamoto, Keiko Takano,* and Yutaka Fukuda*

Department of Chemistry, Faculty of Science, Ochanomizu University, 2-1-1 Otsuka, Bunkyo-ku, Tokyo 112-8610

Received June 8, 2005; E-mail: keiko@cc.ocha.ac.jp

Density functional theory, B3LYP/CEP-31G calculations, were performed on nickel(II) complexes comprising *N*,*N*,*N*′,*N*′-tetramethylethylenediamine (tmen), benzoylacetonate (bzac), and a halide anion (X), Ni(tmen)(bzac)X·n(H_2O) (n = 1–4, X = Cl^-, Br^-, and I^-). Fully optimized geometries of [Ni(bzac)$_2$(tmen)], [NiCl(bzac)(tmen)(H_2O)], and [Ni(bzac)(tmen)(H_2O)$_2$]$^+$ are all in good agreement with crystallographic data. This series of nickel(II) complexes shows a disproportionation reaction in a non-polar and rather inert solvent, such as 1,2-dichloroethane and acetone, accompanied by highly contrasting color changes of the solutions. Also, the presence of an intermediate compound has been confirmed. A possible reaction mechanism of this reaction as well as the structure of the intermediate compound are discussed.

Nickel(II) mixed-ligand complexes are of interest due to their thermochromic and solvatochromic properties, which will lead to their use as thermosensitive coloring matter, various sensors and indicators, particularly as a Lewis-acid–base indicator.[1–3] We recently synthesized a series of nickel(II) complexes comprising of *N*,*N*,*N*′,*N*′-tetramethylethylenediamine (tmen), benzoylacetonate (bzac), and a halide anion (X), Ni(tmen)(bzac)X·n(H_2O) (n = 1–4, X = Cl^-, Br^-, and I^-), and reported on their crystallographic structures, spectral behaviors in various organic solvents, and thermochemical reactions in the solid state.[4] Of particular interest was a disproportionation reaction, which was originally reported by Hoshino et al.,[5] demonstrated by all of these three complexes when they were dissolved in a non-polar and rather inert solvent, such as 1,2-dichloroethane and acetone. During the disproportionation process, octahedral mixed-ligand complexes undergo deaquation and coordination of a halide anion, eventually resulting in two tetrahedral and octahedral complexes, as shown in the following reaction formula (1):

$$2\{\mathrm{Ni(tmen)(bzac)X}\cdot n(\mathrm{H_2O})\} \rightarrow [\mathrm{Ni(bzac)_2(tmen)}] + [\mathrm{NiX_2(tmen)}] + 2n\mathrm{H_2O}. \quad (1)$$

We could confirm the presence of a five-coordinate complex, [Ni(bzac)(tmen)X], as an intermediate in this reaction, through the monitoring of solutions by UV–vis spectroscopy and mass spectroscopy of the thermal-reaction product. However, the spectroscopic data did not allow us to determine the geometry of the intermediate complex; whether it has a square-pyramidal or trigonal-bipyramidal structure.

With the aim of elucidating the structure of this intermediate complex and the reaction mechanism, we report here on the results of a theoretical study performed on this disproportionation reaction.

Computational Details

The effectiveness of the B3LYP hybrid functional based on DFT (density functional theory) for quantum-chemical calculations of transition-metal complexes has been well recognized.[6] Therefore, full-geometry optimizations were performed with the Gaussian 03 program package,[7] at the B3LYP/CEP-31G level of theory on all of the chemical species involved in the disproportionation reaction. In the cases of octahedral, square-pyramidal, trigonal-bipyramidal, and tetrahedral structures, according to the ligand field strength (N_2O_4, N_2O_3, or N_2O_2X donor set) and the degeneracy of the orbitals, a triplet was used to describe the metal's spin state, while a singlet was used for the square-planar geometry. Two structures related to isomerization of the 5-coordinate intermediate complexes, i.e. square pyramidal and trigonal bipyramidal, were further subjected to vibrational frequency calculations at the same level of theory to verify that each of the obtained optimized geometries (stationary points) was a local minimum or a transition state (TS). Full-geometry optimizations starting from appropriate geometries were carried out on [NiCl(bzac)(tmen)(H_2O)],[4] [Ni(bzac)(tmen)(H_2O)$_2$]$^+$ (only the inner coordination sphere of the complex),[4] and [Ni(bzac)$_2$(tmen)][8] for comparisons with the crystallographic data. The complex [NiCl(bzac)(tmen)-(H_2O)] is not involved in the disproportionation reaction of the bromide complex, but is used only to compare an analogous complex with a known crystallographic structure.

Results and Discussion

The optimized structures of [NiCl(bzac)(tmen)(H_2O)], [Ni(bzac)(tmen)(H_2O)$_2$]$^+$, and [Ni(bzac)$_2$(tmen)], together with their ORTEP drawings reported before, are given in Figs. 1, 2, and 3. The calculated bond lengths and bond angles

Published on the web December 9, 2005; DOI 10.1246/bcsj.78.2124

agree very well with the crystallographic data, as listed in Table 1. The DFT calculated bond lengths and bond angles of chemical species involved in the disproportionation reaction are listed in Table 2.

Why is the Disproportionation Reaction of Particular Interest? Nickel(II) complexes are known to have a variety of coordination modes, including octahedral (Oh), square pyramidal, trigonal bipyramidal, square planar (Sp), and tetrahedral (Td). In addition, complexes of one configuration can be easily converted to other configurations, usually accompanied by highly contrasting color changes. A large number of com-

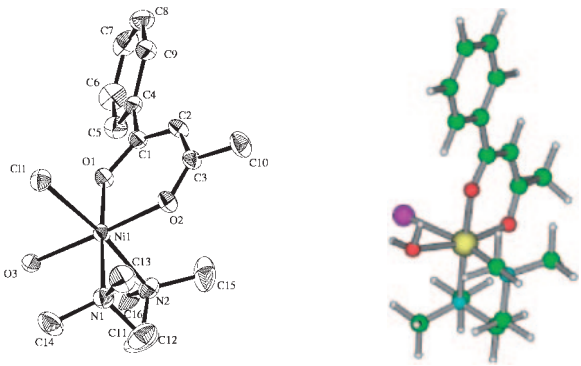

Fig. 1. ORTEP drawing of [NiCl(bzac)(tmen)(H_2O)] (left), and B3LYP/CEP-31G optimized structure (right). In the ORTEP drawing, hydrogen atoms are omitted for clarity. Displacement ellipsoids are drawn at 30% probability.

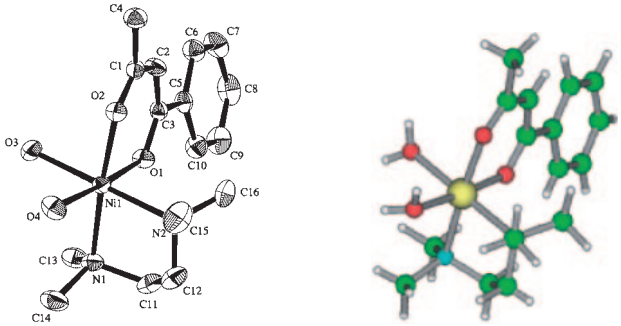

Fig. 2. ORTEP drawing of [Ni(bzac)(tmen)(H_2O)$_2$]$^+$ (left) and B3LYP/CEP-31G optimized geometry (right). In the ORTEP drawing, hydrogen atoms are omitted for clarity. Displacement ellipsoids are drawn at 30% probability.

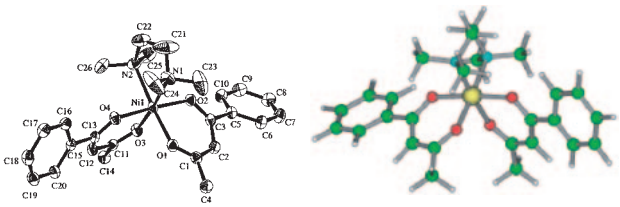

Fig. 3. ORTEP drawing of [Ni(bzac)$_2$(tmen)] (left) and B3LYP/CEP-31G optimized geometry (right). In the ORTEP drawing, hydrogen atoms are omitted for clarity. Displacement ellipsoids are drawn at 30% probability.

Table 1. Selected Bond Lengths (Å) and Angles (°)

Compound		DFT	Crystallographic data
[NiCl(bzac)(tmen)(H_2O)]	Ni–O1	2.04	2.032(3)
	Ni–O2	2.01	2.015(3)
	Ni–N1	2.16	2.195(4)
	Ni–N2	2.20	2.191(5)
	Ni–O3	2.22	2.122(3)
	Ni–Cl	2.52	2.465(2)
	bzac bite	90.1	90.9(1)
	tmen bite	84.8	83.5(2)
[Ni(bzac)(tmen)(H_2O)$_2$]$^+$	Ni–O1	2.01	2.012(2)
	Ni–O2	2.04	2.039(2)
	Ni–O3	2.08	2.081(3)
	Ni–O4	2.12	2.117(3)
	Ni–N1	2.15	2.146(3)
	Ni–N2	2.16	2.161(3)
	bzac bite	89.3	89.31(9)
	tmen bite	84.9	84.8(1)
[Ni(bzac)$_2$(tmen)]	Ni–O1	2.07	2.0323(17)
	Ni–O2	2.05	2.0216(19)
	Ni–O3	2.07	2.0318(18)
	Ni–O4	2.05	2.039(2)
	Ni–N1	2.20	2.160(2)
	Ni–N2	2.20	2.213(2)
	bzac bite 1	88.4	90.24(7)
	bzac bite 2	87.9	89.49(7)
	tmen bite	84.7	82.88(10)

Table 2. B3LYP/CEP-31G Calculated Bond Lengths (Å) and Angles (°) of Chemical Species Involved in the Disproportionation Reaction

	$[Ni(bzac)(tmen)]^+$	[NiBr(bzac)(tmen)]			$[NiBr_2(bzac)(tmen)]^-$
	Square planar	Trigonal bipyramidal	TS	Square pyramidal	Oh
Ni–O1[a)]	1.90	2.03	2.02	2.00	2.00
Ni–O2[a)]	1.90	2.03	2.02	2.00	2.00
Ni–N1[a)]	2.07	2.20	2.15	2.13	2.21
Ni–N2[a)]	2.07	2.12	2.14	2.19	2.20
Ni–Br1		2.50	2.53	2.52	2.82
Ni–Br2					2.94
bzac bite	93.3	87.2	87.7	89.5	93.0
tmen bite	87.3	85.6	84.6	84.1	85.1

a) O1 is the oxygen near the phenyl group, O2 is the oxygen near the methyl group, N1 is the nitrogen at the trans position of the O1, and N2 is the nitrogen at the trans position of the O2.

plexes have been known to show solvatochromic behaviors, but most of the color changes derive from conversion of the coordination modes between Oh and Sp, as did our complex dissolved in nitromethane:

$$[Ni(tmen)(bzac)(H_2O)_2]Br\cdot 2H_2O \rightarrow [Ni(tmen)(bzac)]^+ + Br^- + 4H_2O. \quad (2)$$

If the reaction stops at this stage, it is one of the many solvatochromic examples known so far (conversion from Oh to Sp). However, here the reaction proceeds further for a part of the resulting Sp $[Ni(tmen)(bzac)]^+$ complexes; the negatively charged bromide anion coordinates back to the +1 nickel complex, forming a 5-coordinate intermediate; this intermediate complex then undergoes a disproportionation reaction to provide Td and Oh species (conversion from Sp to Td and Oh via a 5-coordinate intermediate of unknown form). Since the first case was reported,[5] no further work has been undertaken on the disproportionation reaction, and its reaction mechanism is still unknown. With the results of a theoretical study performed on this disproportionation reaction, we have tried to elucidate the structure of this 5-coordinate intermediate complex and the reaction mechanism.

The overall reaction is broken down into 6 continuous steps, and each step is detailed in the next section.

Possible Reaction Mechanisms of the Disproportionation Reaction. Step 1—Dissolution of the Complex: When dissolved in a rather inert and non-polar solvent, $[Ni(bzac)(tmen)(H_2O)_2]Br\cdot 2H_2O$ is dissociated into a complex of +1 by releasing two water molecules of crystallization and Br^-, as follows:

$$[Ni(bzac)(tmen)(H_2O)_2]Br\cdot 2H_2O \rightarrow [Ni(bzac)(tmen)(H_2O)_2]^+ + Br^- + 2H_2O. \quad (3)$$

Since the dissolution of the solid is accompanied by breaking the crystal lattice, the difference in the total energy derived from the DFT calculation is rather irrelevant, and is omitted here. However, once the crystal is dissolved in the solvent, all of the reactions take place in the same system (solution); formulae for Steps 2–6 include the results of DFT calculations.

Step 2—Dehydration: Two aqua ligands attached to the nickel metal ion are then liberated, as shown by the thermochemical equation (4), where the heat of reaction (33.0 kcal mol^{-1}) is obtained as the difference between the sums of the total energies on both sides of the equation to provide the following reaction profile:

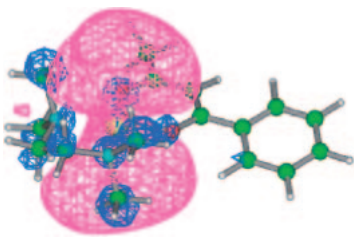

Fig. 4. The second-lowest unoccupied molecular orbital (2nd-LUMO) of $[Ni(bzac)(tmen)]^+$ complex obtained by B3LYP/CEP-31G calculations.

$$[Ni(bzac)(tmen)(H_2O)_2]^+ \rightarrow [Ni(bzac)(tmen)]^+ + 2H_2O + 33.0\,\text{kcal mol}^{-1}. \quad (4)$$

As it shows, this reaction is mildly exothermic, and the complex changes its geometry to Sp with two vacant coordination sites created above and below the plane. These two vacant coordination sites coincide with the second-lowest unoccupied molecular orbital of the $[Ni(bzac)(tmen)]^+$ complex obtained by our DFT calculations. As shown in Fig. 4, this orbital has predominantly the character of the metal $4p_z$ orbital. Table 2 lists that the donor atoms (N1, N2, O1, and O2) located closer to the central metal, than they are in the crystal (Oh geometry) (Table 1). This is consistent with Gutmann's bond-length variation rule.[3]

Step 3—Coordination of Br^-: Br^- shall coordinate to the positively charged metal complex, since both the bromide and the cationic complex are not stabilized in a non-polar solvent. It would be quite natural that the Br^- coordinates to the square-planar Ni complex at a vacant coordination site by occupying the empty orbital shown in Fig. 4, to form a square-pyramidal structure. As shown in the thermochemical equation, this is again an exothermic process:

$$[Ni(bzac)(tmen)]^+ + Br^- \rightarrow [NiBr(bzac)(tmen)] + 92.6\,\text{kcal mol}^{-1}. \quad (5)$$

Due to this change in the coordination mode from Sp to square

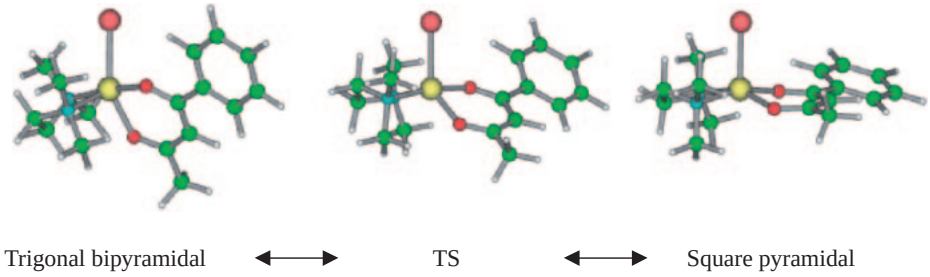

Fig. 5. Isomerization of the 5-coordinate intermediate complexes. Geometries were obtained by B3LYP/CEP-31G calculations.

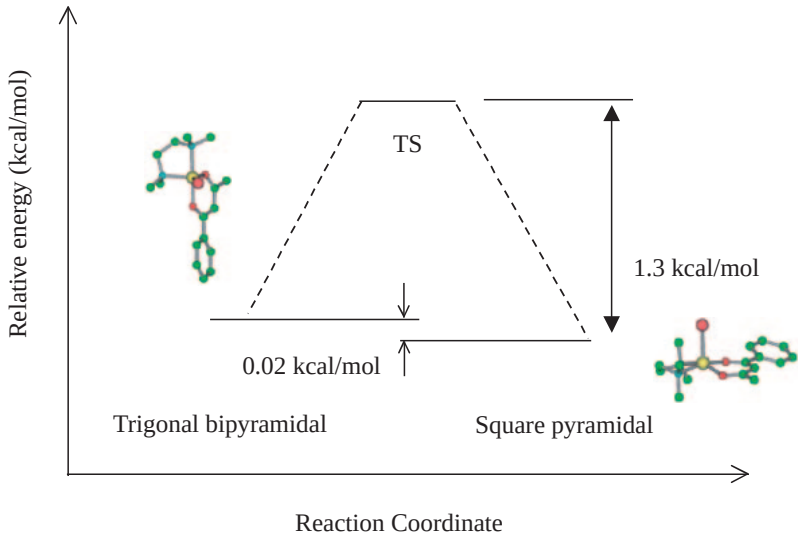

Fig. 6. Energy profile involved in isomerization of 5-coordinate intermediate complexes.

pyramidal, the bond lengths of Ni–O1, Ni–O2, Ni–N1, and Ni–N2 are expected to be increased based on ligand field theory. This has been confirmed by the results of DFT calculations (Table 2).

Step 4—Isomerization: The full-geometry optimization of a square-pyramidal and a trigonal-bipyramidal isomer, followed by a frequency analysis, gave local minimum structures for both geometries (three-dimensional representation of the optimized structures for these two isomers are given in Fig. 5). Their total energies differ only negligibly (see Fig. 6). It is noteworthy that these two isomers are very close in their geometries, as shown schematically in Fig. 7. When nitrogen and oxygen atoms on the equatorial plane of a trigonal-bipyramidal structure (left in Fig. 7) are rotated around the central metal by 30 degrees each, it has a square-pyramidal geometry (right in Fig. 7). A TS search between these two isomers was successful. The TS structure with one imaginary frequency is shown in Fig. 5. The calculated activation energy was 1.3 kcal mol^{-1} for this isomerism. The energy profile given in Fig. 6 indicates that the 5-coordinate intermediate complex can take either the square-pyramidal or the trigonal-bipyramidal structure, since the thermodynamic stabilities of these isomers are nearly the same, and that the isomerization occurs quite freely due to the small activation energy of 1.3 kcal mol^{-1}. Not only as an isolated molecule, but also in the crystal, these two isomers seem to have equal stabilities. Raymond et al. reported that there are two crystallographically

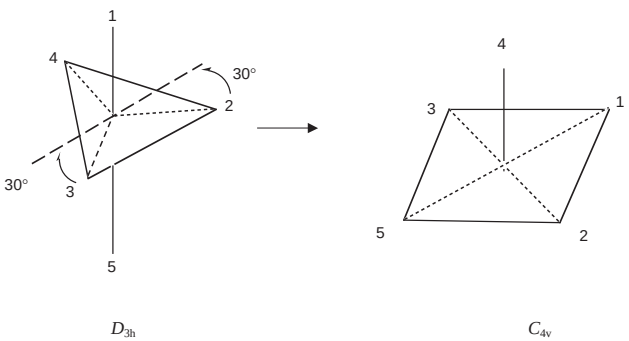

Fig. 7. Schematic view of the structural change from D_{3h} (trigonal bipyramidal) to C_{4v} (square pyramidal).

isolated $[Ni(CN)_5]^{3-}$ ions in the compound of $[Cr(NH_2CH_2CH_2NH_2)_3][Ni(CN)_5]\cdot 1.5H_2O$: one is a regular square pyramid and the other is a distorted trigonal bipyramid.[9]

Step 5—Further Coordination of Br$^-$: There is still another vacant coordination site on the [NiBr(bzac)(tmen)]. Assuming that the Br$^-$ again coordinates to Ni^{2+} at the remaining vacant site, a negatively charged octahedral Ni(II) complex, $[NiBr_2(bzac)(tmen)]^-$, could be formed. Our DFT calculations confirmed that the optimized structure of this hypothetical complex is octahedral, and that the process, as shown in the following thermochemical equation, would be slightly endothermic:

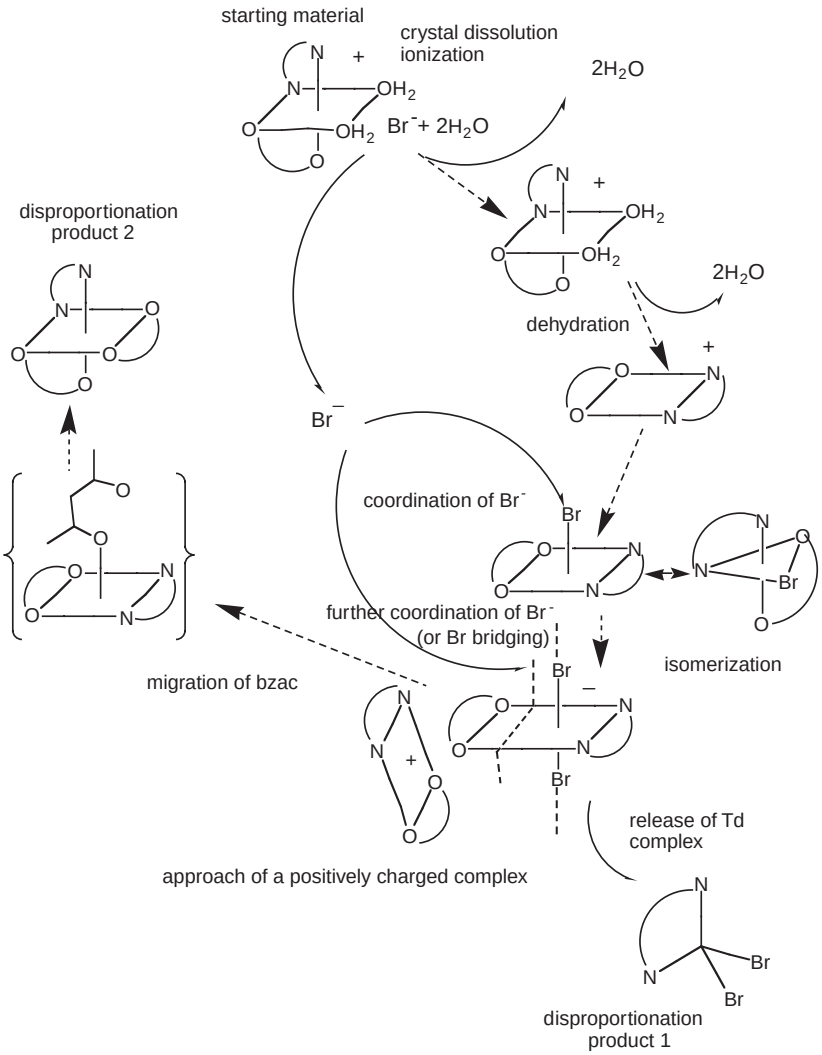

Fig. 8. Overall scheme of the disproportionation reaction.

$$[\mathrm{NiBr(bzac)(tmen)}] + \mathrm{Br}^- \rightarrow [\mathrm{NiBr_2(bzac)(tmen)}]^- - 13.2\,\mathrm{kcal\,mol^{-1}}. \quad (6)$$

The coordination of the additional Br^- does not affect the bond lengths between the nickel and the in-plane donor atoms, and only the Ni–Br distance is extended (Table 2) compared to the square-pyramidal structure. In an actual solution, however, several 5-coordinate complexes may be linked together to form one-dimensional bromide bridged Ni complexes, $\{-[\mathrm{NiBr(bzac)(tmen)}]-\}_m$ (m = integer), as is seen in $[\mathrm{Ni^{III}(chxn)_2Br}]\mathrm{Br_2}$ (chxn = cyclohexanediamine).[10] This one-dimensional structure is more advantageous in the non-polar solvent than the hypothetical octahedral structure of the Ni(II) complex, $[\mathrm{NiBr_2(bzac)(tmen)}]^-$, since the former complex is chargeless, and more stable than the chargeless 5-coordinate complex, because the Oh geometry around the nickel is energetically more advantageous than the 5-coordinate species from the viewpoint of the structural preference energies.[11]

Step 6—Migration of Benzoylacetonato and Release of $[NiBr_2(tmen)]$: In the solution, the above-mentioned Br-bridged complex chain has a negatively charged end that attracts the cationic complex $[\mathrm{Ni(bzac)(tmen)}]^+$. On the other hand, four electronegative atoms ($2Br^-$ and $2O^-$) in the $[\mathrm{NiBr_2(bzac)(tmen)}]^-$ moiety are naturally repelling each other. Therefore, if the cationic complex comes closer to the negatively charged side of the complex chain, one of the benzoylacetonato's oxygen atoms may be repelled from the anionic $[\mathrm{NiBr_2(bzac)(tmen)}]^-$ moiety and coordinate to the metal of the cationic complex; i.e. benzoylacetonato will be eventually cut off from the chain to leave a tetrahedral $[\mathrm{NiBr_2(tmen)}]$ complex behind, and to produce an octahedral $[\mathrm{Ni(bzac)_2(tmen)}]$ complex, as expressed in the following thermochemical equation (7) (see Fig. 8):

$$[\mathrm{NiBr_2(bzac)(tmen)}]^- + [\mathrm{Ni(bzac)(tmen)}]^+ \rightarrow [\mathrm{NiBr_2(tmen)}] + [\mathrm{Ni(bzac)_2(tmen)}] + 81.2\,\mathrm{kcal\,mol^{-1}}. \quad (7)$$

It should be noted that the coordination of benzoylacetonato to the square-planar complex $[\mathrm{Ni(bzac)(tmen)}]^+$ is a "no barrier reaction." An optimization calculation starting from a hypothetical intermediate structure of $[\mathrm{Ni(bzac)_2(tmen)}]$ (shown in curly brackets in Fig. 8, in which only one of the oxygens

of benzoylacetonato is coordinated to the central metal) resulted in exactly the same octahedral geometry as that from the optimization calculation performed separately (the result of which is shown in Table 1).

Effect of Asymmetry of Benzoylacetonate. Since benzoylacetonate is not a symmetrical ligand, due to its methyl and phenyl groups, we optimized the other structure of [NiCl(bzac)(tmen)(H_2O)] having the benzoylacetonate in a different orientation (in which the phenyl group attaches to the opposite carbon atom). There was little difference in the energy between these two isomers; it therefore appears that the position of the phenyl and methyl substituents of the benzoylacetonato does not affect the stability in this complex. Although these two isomers have nearly the same thermodynamic stabilities as an isolated molecule, interestingly, only one of these isomers is found in the crystal. The reason is still unknown and needs further investigation. It may be related to the crystal packing as these chloride complexes form dimers in crystals by hydrogen bonding.[4]

Conclusion

A possible reaction mechanism for the disproportionation reaction was discussed and presented with the reaction profile obtained from DFT calculations. The DFT optimized structures of [Ni(bzac)$_2$(tmen)], [NiCl(bzac)(tmen)(H_2O)], and [Ni(bzac)(tmen)(H_2O)$_2$]$^+$ are all in good agreement with the crystallographic data. DFT calculations were also an effective tool for elucidating the structure of the intermediate complex with the energy profile involved in isomerization. Two isomers of the 5-coordinate intermediate complex in the disproportionation reaction were found to have almost identical thermodynamic stabilities, and isomerization between these two species seems to take place quite freely due to the small activation energy of 1.3 kcal mol^{-1}. Although the two isomers of the chloro complex [NiCl(bzac)(tmen)(H_2O)] with different benzoylacetonato orientations have almost the same thermodynamic stabilities as an isolated molecule, interestingly, only one of them occurs in crystals.

References

1 K. Sone and Y. Fukuda, *Rev. Inorg. Chem.*, **11**, 123 (1990).

2 W. Linert, R. F. Jameson, and A. Taha, *J. Chem. Soc., Dalton Trans.*, **1993**, 3181.

3 V. Gutmann, "The Donor–Acceptor Approach to Molecular Interactions," Plenum Press, New York, London (1978).

4 K. Miyamoto, M. Sakamoto, C. Tanaka, E. Horn, and Y. Fukuda, *Bull. Chem. Soc. Jpn.*, **78**, 1061 (2005).

5 N. Hoshino, Y. Fukuda, and K. Sone, *Bull. Chem. Soc. Jpn.*, **54**, 420 (1981).

6 S. Okeya, K. Wakamatsu, T. Shibahara, H. Yamakado, and K. Nishimoto, *J. Comput. Chem. Jpn.*, **1**, 97 (2002), and the references cited therein.

7 M. J. Frisch, G. W. Trucks, H. B. Schlegel, G. E. Scuseria, M. A. Robb, J. R. Cheeseman, J. A. Montgomery, Jr., T. Vreven, K. N. Kudin, J. C. Burant, J. M. Millam, S. S. Iyengar, J. Tomasi, V. Barone, B. Mennucci, M. Cossi, G. Scalmani, N. Rega, G. A. Petersson, H. Nakatsuji, M. Hada, M. Ehara, K. Toyota, R. Fukuda, J. Hasegawa, M. Ishida, T. Nakajima, Y. Honda, O. Kitao, H. Nakai, M. Klene, X. Li, J. E. Knox, H. P. Hratchian, J. B. Cross, C. Adamo, J. Jaramillo, R. Gomperts, R. E. Stratmann, O. Yazyev, A. J. Austin, R. Cammi, C. Pomelli, J. W. Ochterski, P. Y. Ayala, K. Morokuma, G. A. Voth, P. Salvador, J. J. Dannenberg, V. G. Zakrzewski, S. Dapprich, A. D. Daniels, M. C. Strain, O. Farkas, D. K. Malick, A. D. Rabuck, K. Raghavachari, J. B. Foresman, J. V. Ortiz, Q. Cui, A. G. Baboul, S. Clifford, J. Cioslowski, B. B. Stefanov, G. Liu, A. Liashenko, P. Piskorz, I. Komaromi, R. L. Martin, D. J. Fox, T. Keith, M. A. Al-Laham, C. Y. Peng, A. Nanayakkara, M. Challacombe, P. M. W. Gill, B. Johnson, W. Chen, M. W. Wong, C. Gonzalez, and J. A. Pople, "Gaussian 03, Revision B.03," Gaussian, Inc., Pittsburgh PA (2003).

8 K. Miyamoto, F. Murata, E. Horn, and Y. Fukuda, *Z. Kristallogr.—New Cryst. Struct.*, **220**, 31 (2005).

9 K. N. Raymond, P. W. R. Corfield, and J. A. Ibers, *Inorg. Chem.*, **7**, 1362 (1968).

10 K. Toriumi, Y. Wada, T. Mitani, S. Bandow, M. Yamashita, and Y. Fujii, *J. Am. Chem. Soc.*, **111**, 2341 (1989).

11 K. F. Purcell and J. C. Kotz, "Inorganic Chemistry," W. B. Saunders Company, Hong Kong (1977).